Effect of Graphene and Fe_3O_4 on the Protection Efficiency of Polyeugenol Conducted Coating for Stainless Steel 316L in NaCl solution

Khulood Abid Saleh ID ✉, *Ayat Monther Alqudsi** ID ✉

Department of Chemistry, College of Science, University of Baghdad, Baghdad, Iraq.
*Corresponding Author.

Abstract

Corrosion is the term for the surface disintegration of metals and alloys in a specific environment. Corrosion processes change a metal alloy's chemical properties as well as its mechanical behaviors. To stop rusting, a novel strategy based on an original material has been applied. By electrochemically synthesizing polyEugenol(PE)/nanocomposite (Grapgene,Fe3O4) on stainless steel 316L (SS316L), which serves as the working electrode, using the electropolymerization approach, conducting polymer-composites are material types that show promise for anticorrosion. The atomic force microscopy images (AFM) and Fourier transform-infrared spectroscopy analyses were used to evaluate the produced coated polymer. The results showed that, in comparison to the blank SS316L, PE/Nanocomposite and PE offer the metal's best corrosion protection

Keywords: Corrosion, Electro polymerization, Eugenol, Nanocomposite, Polyeugenol.

Introduction

The use of biobased molecules obtained from renewable sources to substitute petroleum-based ones for manufacturing products is actively promoted due to current environmental concerns and legislation.[1,2] . A desirable alternative for the production of green polymers is the use of biobased monomers in polymerization. A fascinating chemical for the creation of biobased monomers and polymers is eugenol, a naturally occurring phenol that is now mostly derived from clove oil but might potentially be made by depolymerizing lignin. By altering the phenol group, it is simple to insert readily polymerizable functional groups into the chemical structure[3].

Due to its simplicity and repeatability, the electro-chemical polymerization process is a common methodology that is frequently utilized for the creation of electro-active conducting polymer films [4]. Potentiostatic, galvanostatic, potential step, and potential sweep methods are often used in the electropolymerization of monomers and their derivatives[5]. The features and applications of the polymer films produced are therefore influenced by the type of the monomer, pH, solvent effect, temperature, applied potential, doping effect, electrolyte solution, direction of potential sweep, and voltammetry potential window[6]. In essence, this procedure entails providing a voltage to an anode (working electrode) that is positioned inside an electrochemical cell that also includes an electrolyte

solution, a doping agent (if required), and a monomer. Free radicals might then be created by electrochemically oxidizing the monomer. Two important subgroups of the electrochemical polymerization process are anodic and cathodic electrochemical polymerization[7].

From cloves of the Syzygium genus, eugenol, or "4-allyl,2-methoxyphenol," an important phenol compound, is synthesized. It is an adaptable natural material that may possess a number of beneficial properties, including anti-inflammatory, antioxidant, and antibacterial effects. Eugenol is also widely known to be advantageous as a local anesthetic in dentistry due to its capacity to lessen tooth pain by blocking the voltage-gated sodium channel (VGSC) and activating the transient receptor potential vanilloid subtype (TRPV1). [8,9] The conventional application of eugenol as a local anesthetic in a painful area like intact skin has been curtailed due to its negative side effects.

According to Al-Mashhadani, H. A., & Saleh, K. A, Before and after Micro Arc oxidation, Eugenol polymerized on titanium alloys had high protection efficacy (Pe%) at 323K and was resistant to corrosion. Thus, the efficiency increased to 81%. The samples' ability to fight against numerous oral bacteria and fungi was assessed. In addition to having antibacterial effects against S. aureus and B. subtilis, the Poly Eugenol (PE) coating has antifungal efficacy against C. albicans and C. glabrata oral fungus[10]. By electropolymerizing Eugenol oxidative polymerization on a platinum electrode.

Basid et al. investigate polyeugenol/graphene composite as a corrosion-prevention coating. The barrier properties of graphene can significantly improve the corrosion resistance of metals connected to polymers. Polyeugenol (PE) was created using the cationic addition polymerization process. When 1.25% graphene by weight was added to the PE polymer matrix, the corrosion protection efficacy increased from 37% to 78%, making the PE/G composite more corrosion-resistant than pure PE. [11]. To assess PE's antibacterial and antioxidant properties, Erwin A. produced a high molecular weight version, which was then measured using a viscometer. Those findings showed a strong antibacterial action. Testing of antioxidant defenses from DPPH, as a free radical, followed by diphenyl pycrylhydrazyl . As a result, the synthetic polyeugenol offers a great deal of promise for use in numerous biological applications [12].

In this work, stainless steel 316L (SS316L) alloys are electropolymerized by forming layer of polyeugenol (PE) on the surface of the alloy using an alkaline electrolyte than the effect of Graphene and Fe_3O_4. The electrosynthesis of PE coatings was examined using FT-IR spectroscopy and AFM measurements, and the coating adhesive was assessed to ascertain their surface morphologies. Investigations were also done on the biological effectiveness of PE covering against oral fungi and bacteria.

Materials and Methods

Stainless Steel alloys (SS 316 L) specimens of 2×2 cm^2 area area (including 0.08 weight percent (Wt%) (C), > 0.75 Wt% (Si), 2.00 Wt% (Mn), 17.00 Wt% (Cr), > 0.045 Wt% (P), 12.00 Wt% (Ni), 0.030 Wt% (S), 2.5 Wt% (Mo), 0.10 Wt% (N) and iron (Fe) the remaining to 100% from 31.00-38.00) were purchased from commercial sources SS 316L alloy of (0.5) mm thickness, These samples were had been polished using emery sheets of various grades, including 600, 800, 1200, and 2000 mesh grit, and then washed with tap water, distilled water, ethanol, and lastly acetone before being dried by hot air drier. The materials used are listed in the Table 1 below

Table 1. List of required chemicals

Raw Material	Molecular Formula	Supplier	Purity
Eugenol	$C_{10}H_{12}O_2$	MASTER-DENT	99%
Ethanol	C_2H_5OH	GCC	99.9%
Oxalic acid	$H_2C_2O_4$	BDH	99%
Di - Methyl Sulfoxide	$(CH_3)_2SO$	LOBA Chemie	98%
Sodium Chloride	NaCl	BDH	99.5%
Sulfuric acid	H_2SO_4	GCC	98%
Sodium hydroxide	NaOH	BDH	99%
Graphene	G	Hongwe nanometer	99%
Ferrous oxide	Fe_3O_4	Hongwe nanometer	99%

Cyclic Voltammetry is used to determine the electro polymerization potential. A solution of 10mM Eugenol in 70% 0.1M NaOH solution was prepared with a few drops of concentrated H_2SO_4 added to improve electrolyte conductivity between a voltage range from -2000 mV to 2000 mV vs. a typical calomel electrode. the consecutive cyclic voltammogram made using PE at around 2.8 volts.

Euginol Electrochemical Polymerization

A cell contains two electrodes, the first working electrode which is made of stainless steel 316L, and the second electrode is the counter electrode which is made of graphene rode. The first electrode acts as an anode and the second acts as a cathode.

To prepare a protected film of poly eugenol on the SS316L, a (10 Mm) solution of eugenol was prepared in (0.1 M) of NaOH solution with a few drops of sulphuric acid and 0.1g of oxalic acid. The work was achieved at room temperature and by applying 2.8volt and at 90 min. Finally, the surface is cleaned, washed with distilled water then dried by hot dry air[13] .Eq. 1 shows how the monomer electrochemically polymerizes.

...1
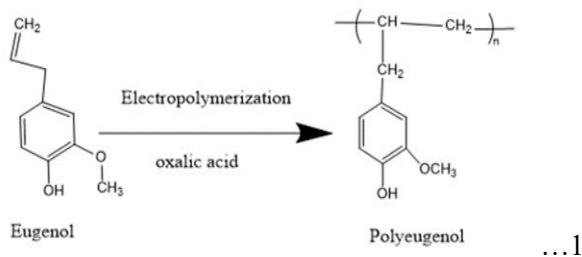
Results and Discussion

Corrosion studies
Fig. 2 depicts typical polarization curves for coated and uncoated stainless steel type 316L with prepared polymer before and after using nanomaterial in a 3.5% solution of sodium chloride with 298-328 K of temperature range. The following Eq. 2 is used to determine the protection efficacy [14,15]

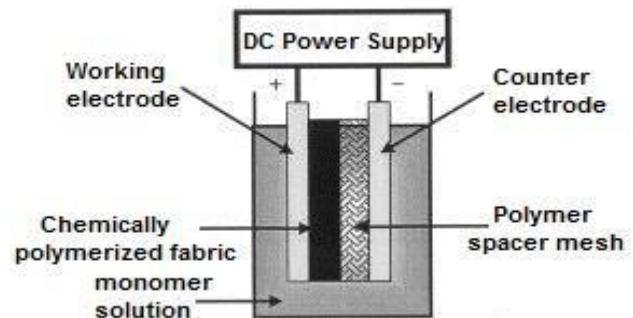%Pe =[(I$_{cor.}$)$_{unc.}$-(I$_{cor.}$)$_{c.}$]/ (I$_{cor.}$)$_{unc.}$ …… **2**

Figure 1. Electropolymerization system

To increase the polymer film's resistance to corrosion and bacteria, (0.01, 0.02, 0.01, 0.03, and 0.04)g of nanomaterial (G and Fe_3O_4) are added in this phase. The measurements from the Tafel plots indicated that 0.02g of both G and Fe_3O_4 was the optimal amount. Hence, the following procedures for electro polymerization were followed when nanomaterials were present: , a (10 Mm) solution of eugenol was prepared in (0.1 M) of NaOH solution with a few drops of sulphuric acid and 0.1g of oxalic acid and 0.02g of G and Fe_3O_4 Severally. The work was achieved at room temperature and by applying 2.8volt and at 90 min. Finally, the surface was cleaned, washed with distilled water then dried by hot dry air. The electro polymerization system is shown in Fig. 1.

Where (I$_{cor.}$)$_{unc.}$ And (I$_{cor.}$)$_{c.}$ are the corrosion current density for blank SS316L(uncoated) and for coated SS316L, derived by extrapolating the corrosion potential from the cathodic and anodic Tafel lines. The rearranged Stern-Geary equation may be used to calculate the polarization resistance (Rp).[16]

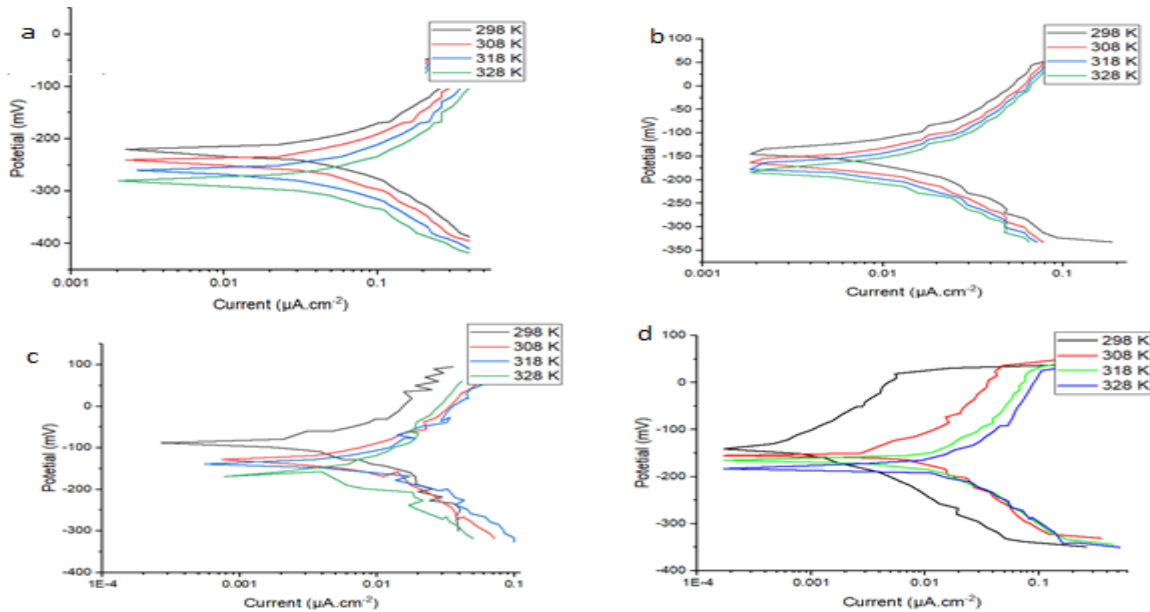$$Rp = \frac{\beta a * \beta b}{(\beta a + \beta b) 2.303} * \frac{1}{Icor} \quad \cdots\cdots\cdots \quad 3$$

Figure 2. Shows the Tafel curves for corrosion of the following materials: a.untreated alloy, b. coating PE, c. coating PE/ G, and d. coating PE/Fe₃O₄.

The cathodic and anodic Tafel plots in a solution of 3.5% NaCl were used to calculate the corrosion potential (Ecor) and corrosion current density (Icor) of the SS316L that had not been coated with PE before to and after. Using Fig. 4, it was also possible to determine polarization resistance Rp, the weight loss WL, protection efficiency Pe% and penetration loss PL. According to Table 2 findings, temperature enhanced the corrosion potential and current density. Tafel's graphic illustrates how the coated alloy gives E_{cor}. Climbs to higher values as compared to uncoated SS316L, demonstrating how the coating acts as an anodic barrier.[17]

Table 2. Corrosion values for polymer PE-coated and untreated SS316L.

system	T(K)	$-E_{COR.}$ (mV)	$I_{COR.}$ ($\mu A/cm^2$)	$-\beta c$ (mV/Dec)	βa (mV Dec)	WL ($g/m^2.d$)	Rp (Ω/cm^2))	PL (mm/y)	PE%
Uncoated	298	219	32.78	123	102	8.22	738.6	0.36	
SS316L	308	242	76.79	175	173	12.9	491.9	0.85	
	318	260	88.83	164	182	22.3	421.6	0.99	
	328	278	127.69	179	186	31.3	310.1	1.39	
Coated	298	145	5.73	114	111	1.44	4261.8	$6.39*10^{-2}$	82.5
$P_{Eugenol}$	308	163	10.48	172	160	2.63	3434.4	0.117	86.3
	318	178	20.76	121	111	2.98	1210.8	0.13	76.6
	328	184	35.54	166	186	3.07	1071.6	0.25	72.1
Coated	298	88	0.56	79.1	78.6	$0.56*10^{-1}$	30569.2	$0.25*10^{-2}$	98.2
$P_{Eugenol}+G$	308	128	0.87	73.6	75.3	$1.73*10^{-1}$	18576.5	$0.77*10^{-2}$	98.8
	318	139	1.44	75.6	73.8	$3.62*10^{-1}$	11260.8	$1.61*10^{-2}$	98.3
	328	169	2.85	75.9	72.2	$4.62*10^{-1}$	5637.4	$2.06*10^{-2}$	97.7
Coated	298	141	1.03	103	111	0.21	22522.4	$0.54*10^{-2}$	96.8
$P_{Eugenol}+Fe_3O_4$	308	155	3.33	121	113	0.83	7619.2	$3.71*10^{-2}$	95.6
	318	165	8.76	101	109	2.20	2598.5	$9.78*10^{-2}$	90.1
	328	183	11.83	102	105	2.96	1899.06	$13.2*10^{-2}$	90.7

The parameters for measuring polarization resistance (Rp) values listed in Table 2 are similar to those for measuring by the polarization curves. Also, they offer a useful method for identifying corrosion disturbances and initiating remedial action.

According to these findings, rate variations that govern the steps in the metal dissolution reaction range from electrochemical desorption and chemical desorption in cathodic reactions through the charge transfer process. At all temperatures, there are variations in the anodic and cathodic Tafel slope findings.[18]. The values of polarization resistance Rp for uncoated and coated SS316L without and with nanomaterials decreased with temperature, as shown in Tables.2 and calculated from Eq. 3. because polymer layers are less conductive than bare metal [19]. This is due to the nanoparticles' virtually full coverage of the SS316L surface. The electropolymerization of eugenol in the presence of

G in a NaCl at 298 K also has the highest Rp rating (30569 /cm^2). According to Table.2's findings, temperature has a significant impact on protection efficiency (Pe%), and Pe% decreases with temperature rises. The fact that temperature-dependent increases in boundary layer thickness occurred can serve to illuminate this. [20].

FTIR Spectroscopy of the polyeugenol (PE) FT-IR spectra for the polyeugenol and eugenol monomer produced on an SS 316L alloy by electrochemical polymerization were captured as shown in Fig. 3a. The asymmetric =CH$_2$ in eugenol is attributed to the absorption bands at 3076 cm^{-1} in Fig. 3b although the polyeugenol IR spectra do not show this peak. The peak at about 3299 cm^{-1}, which is not present in the IR spectra of eugenol, is due to intramolecular H-bonds between the polyeugenol chins' repeating units[21].
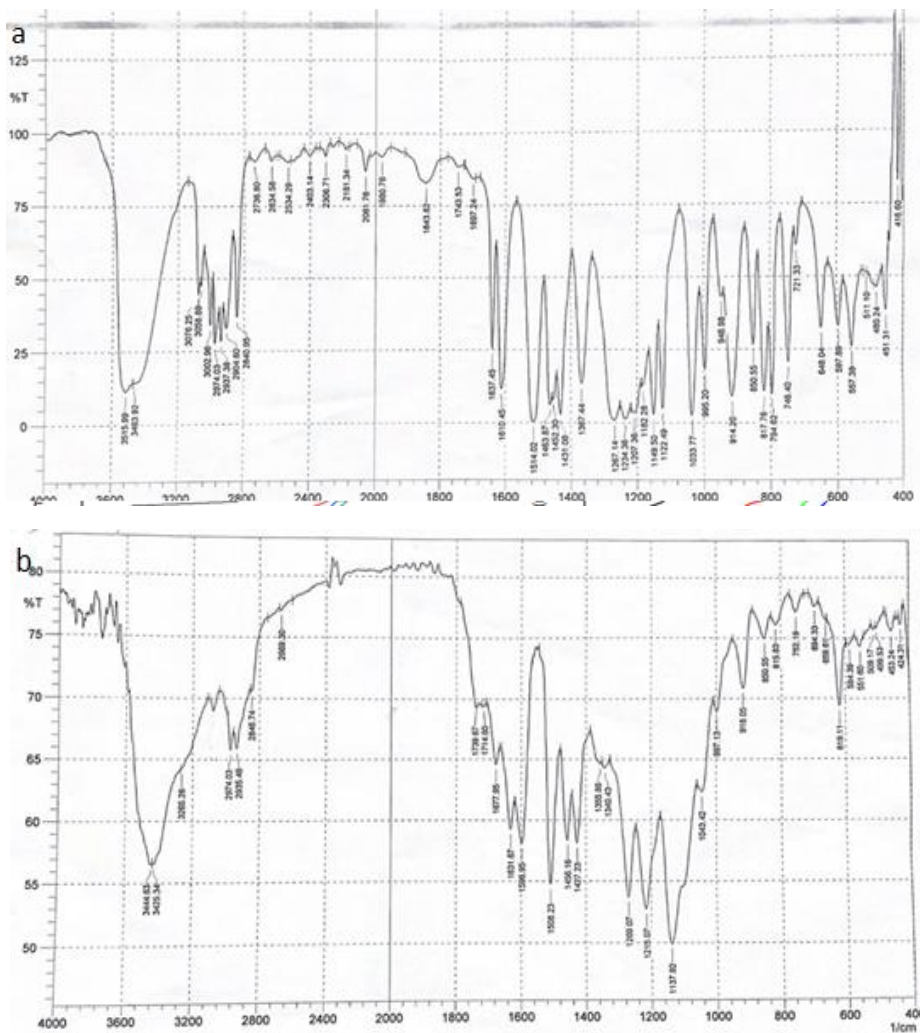

Figure 3. FTIR spectra of a.eugenol b.PE

Using a comparable Arrhenius formula as following Eq. 4[22]

$$I_{cor.} = A \exp^{-Ea/RT} \dots\dots \quad 4$$

By the temperature range 298-328 K , the corrosion treatment of SS316L that for coated and uncoated alloy in a 3.5 percent NaCl solution were determined.

The resulting logarithmic version of the Eq.5 is as follows.

$$\text{Log } I_{cor.} = \text{Log } A - Ea/(2.303RT) \dots\dots \quad 5$$

whereas the following, is the transition state equation[23] as Eq. 6

$$\text{Log } (I_{cor.})/T = \text{Log } [R/Nh] + \Delta S^*/(2.303R) - \Delta H^*/(2.303RT) \dots\dots \quad 6$$

Where h is the Planks constant and has the value $6.62*10^{-34}$ J S, R is the universal gas constant and has the value 8.31 J/K.mol, the absolute temperature (T) in K, A is the preexponential factor, N is the Avogadros number and has the value $6.02*10^{23}$ mol, The thermodynamic functions are ΔS and ΔH (entropy and enthalpy of activation), and E_a is the activation energy. The slope and intercept of the linear regression between Log $I_{cor.}$ vs. 1/T produced the E_a and A values, as shown in Fig. 4a. ΔH and ΔS were determined using the linear regression's slope

and intercept between Log Icor./T and 1/T., as shown in Fig. 4b and summarized in Table 3.
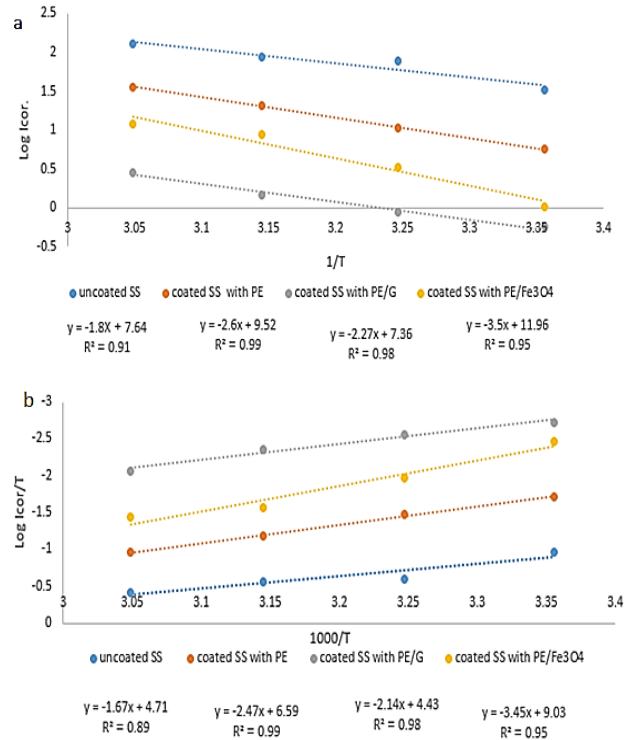

Figure 4. A graph showing: a. log Icor. Against 1/T for SS316L with coating by PE/G, Fe₃O₄ , b. log $I_{cor.}$/T versus 1000/T SS316L for with coating by PE/G, Fe₃O₄.

Table 3. The kinetic and thermodynamic parameters for SS316L with coating by PE/G, Fe₃O₄.

system	Enthalpy ΔH (KJ/mol)	Entropy–ΔS (J/mol.K)	Activation energy Ea (kJ/mol)	A (Molecule.Cm⁻² .S⁻¹)
uncoated SS316L alloy	31.98	107.43	34.47	$26.29*10^{30}$
Coated SS316L coated by PE	47.30	71.43	49.79	$1.99*10^{33}$
Coated SS316L by PE/G	84.83	156.56	67.03	$5.49*10^{35}$
Coated SS316L by PE/Fe₃O₄	40.98	112.79	43.47	$13.79*10^{31}$

The calculated values of the kinetics and thermodynamic parameters are all included in Table 3. The results show that the value of activation energy rose after coating by polyeugenol, indicating a better coating's effectiveness as a barrier. Additionally, the values of the Arrhenius factor, can determine how many corrosion locations are present on the alloy. It noticed that the activation energy after coating has increased, which means that the energy barrier for the reaction process is high[24], making the coating process difficult despite the increase in the value of A (Arrhenius factor) and that means

increased corrosion sites but the higher Ea value helped to increase corrosion protection.

The endothermic properties of St.transition St's state reaction are demonstrated by positive values of enthalpies (ΔH*) for both uncoated and coated stainless steel SS 316L. The fact that both coated and uncoated SS316L exhibit negative values for ΔS* indicates that instead of being a dissociation, the activation complex during the speed determination phase is a combination. This suggests that the degree

of disordering decreases as one moves from a reactant to an activated complex[25].

AFM for PE, PE/G and PE/ Fe₃O₄

Using the AFM Technique, the surface topography and morphology of SS316L coated with PE was investigated both in the presence and absence of nanoparticles (Fe₃O₄ and G). Fig. 5 displays 2D and 3D AFM images of every coating film that has been used. The three most used metrics for assessing a surface's roughness using AFM-analysis are : Ra is the mean grain size ,Rq is the root mean square, and the roughness average. According to findings, as shown in Table 4. The use of nanoparticles to reduce the grain size of PE resulted in a reduction in surface roughness for all coated films. Therefore, the less rough the surface, the greater the barrier effect for avoiding coating corrosion [26,27]

Table 4: AFM parameters to blank and coated SS316L with PE and PE/G, Fe₃O₄

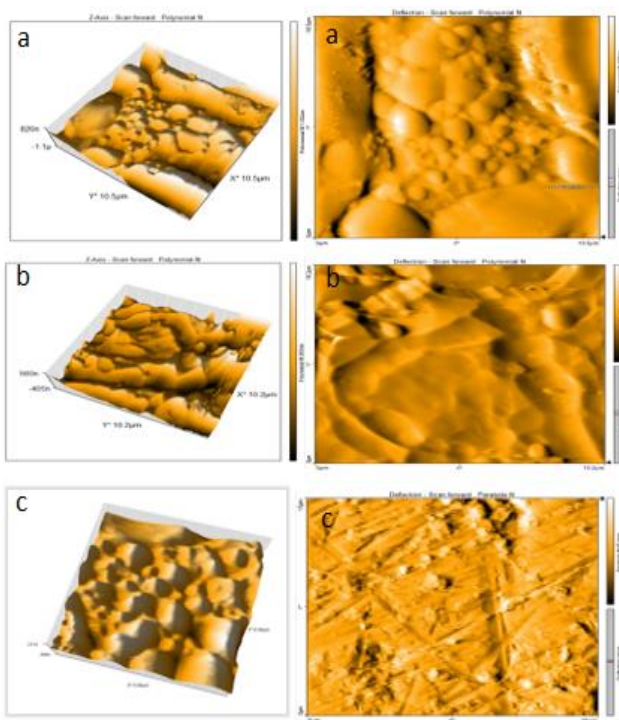| Samples	Ra (nm)	Rq (nm)	mean grainsize (nm)
With coating of PE	42.9	54.11	206.5
coated of polymer PE modified by G	21.65	32.58	234.1
coated of polymer PE modified by Fe₃O4	32.50	53.98	221.76

Figure 5. AFM Images of,   a. PE, b. PE/G, c. PE/Fe₃O₄.

PE's antimicrobial properties

In two cases, the inhibitory zones of the synthesized polymers were tested against S. aureus and E. coli in both the presence and absence of the nanomaterials G and Fe₃O₄ at 800 g/ml. As a solvent, di-methyl sulfoxide was used. (DMSO). The results are summarized in Table 5.

Table 5. The PE and PE/G, Fe₃O₄ inhibition zone.

The sample	gram positive (S. aureus)	gram negative (E. coli)
Polymer of PE	12	16
Polymer of PE/G	26	24
Polymer o PE/Fe₃O₄	24	25
Amoxicilline	30	30
di-methyl sulfoxide	-	-

The produced polymers showed greater inhibitory efficacy toward *S.aureus* and *E.coli* when compared to *amoxicillin*. The polymer's ability to kill bacteria is determined by the stable interaction complex produced between the cleaved DNA and the drug-bound topoisomerases.. The polymer's suppression of topoisomerase activity and the formation of stable complexes with DNA have a significant detrimental effect on cells, as shown by the cell's resistance to medicines that damage DNA[28]As an antibacterial strategy to combat the spread of communicable diseases and the emergence of antibiotic-resistant strains, nanomaterials are taking on a larger role in pharmaceutical and biological applications[29]. Nanomaterials are thought to interact closely with microbial membranes due to their tiny size, high surface-to-volume ratio, and high surface area.

Conclusion

Electropolymerization of PL on SS316L produced a potent anti-corrosion coating in a 3.5% NaCl solution. The coated polymer's protection effectiveness (Pe%) and polarization resistance (Rp) both decline as temperature rises, but the Pe% rises when nanomaterials, notably Graphene, are added. Anodic protection is provided as a result of the change in the corrosion potential to the noble side.

The establishment of a protective layer on the surface of the SS316L is related to the examined SS316L protection, claims the FAM research. Additionally, Gram positive bacteria (B. subtilis) and Gram negative bacteria (E. coli) do not respond well to the antibacterial properties of the polymer film (PE) covered with nanomaterial (S. aureus).

Acknowledgment

Authors' Declaration

- Conflicts of Interest: None.
- We hereby confirm that all the Figures and Tables in the manuscript are ours. Furthermore, any Figures and images, that are not ours, have been included with the necessary permission for re-publication, which is attached to the manuscript.

- Ethical Clearance: The project was approved by the local ethical committee at University of Baghdad.
- Ethics statement:
  No animal studies are present in the manuscript.
  No human studies are present in the manuscript.
  No potentially identified images or data are present in the manuscript.

Authors' Contribution Statement

Data was gathered, examined, and outcomes were interpreted by A. M. N., and the research plan was created, results were tracked, and the manuscript was proofread by K. A. S.

References

1. Tenorio-Alfonso A, Sánchez MC, Franco JM. A review of the sustainable approaches in the production of bio-based polyurethanes and their applications in the adhesive field. J Polym Environ. 2020; 28: 749-74. https://doi.org/10.1007/s10924-020-01659-1
2. Hamed I, Jakobsen AN, Lerfall J. Sustainable edible packaging systems based on active compounds from food processing byproducts: A review. Compr Rev Food Sci. 2022; 21(1): 198-226. https://doi.org/10.1111/1541-4337.12870.
3. Molina-Gutiérrez S, Ladmiral V, Bongiovanni R, Caillol S, Lacroix-Desmazes P. Emulsion polymerization of dihydroeugenol-, eugenol-, and isoeugenol-derived methacrylates. J Ind Eng Chem. 2019; 58(46): 21155-64. https://doi.org/10.1021/acs.iecr.9b02338.
4. Zhao Y, Nakanishi S, Hydroxylated and aminated polyaniline nanowire networks for improving anode performance in microbial fuel cells J Biosci Bioeng.

2011; 112(1) :63-6. https://doi.org/10.1016/j.jbiosc.2011.03.014
5. Gupta R, Singhal M, Nataraj SK, Srivastava DN. A potentiostatic approach of growing polyaniline nanofibers in fractal morphology by interfacial electropolymerization. . RSC Adv. 2016; 6(111): 110416-21, https://doi.org/10.1039/C6RA21759A
6. Heinze J, Frontana-Uribe BA, Ludwigs S. Electrochemistry of Conducting Polymers☐ Persistent Models and New Concepts. Chem Rev. 2010; 110(8): 4724-71.https://doi.org/10.1021/cr900226k.
7. Das TK, Prusty S. Review on conducting polymers and their applications. Polym Plast Technol Eng. 2012; 51(14):1487-500 https://doi.org/10.1080/03602559.2012.751410
8. Cherdchom S, Keawsongsaeng W, Buasorn W, Rimsueb N, Development of Eugenol-Embedded Calcium Citrate Nanoparticles as a Local Anesthetic Agent. ACS omega. 2021; 6(43): 28880-28889. https://doi.org/10.1021/acsomega.1c03831

9. Prasad S N. Neuroprotective efficacy of eugenol and isoeugenol in acrylamide-induced neuropathy in rats: behavioral and biochemical evidence. Neurochem. Res. 2013; 38(2): 330-345. https://doi.org/10.1007/s11064-012-0924-9

10. Al-Mashhadani H A, Saleh K A. Electropolymerization of poly Eugenol on Ti and Ti alloy dental implant treatment by micro arc oxidation using as Anti-corrosion and Anti-microbial. Res J Pharm Technol. 2020; 13(10): 4687-4696. https://doi.org/10.1007/s11064-012-0924-9

11. Prasetya, NBA, Ajizan AI, Widodo DS, Ngadiwiyana N, Gunawan G. A polyeugenol/graphene composite with excellent anti-corrosion coating properties. Adv Mater Technol. 2023; 4(1): 248-255. https://doi.org/10.1039/D2MA00875K

12. Rahim E A, Istiqomah N, Almilda G, Ridhay A, Sumarni NK, Indriani I. Antibacterial and Antioxidant Activities of Polyeugenol with High Molecular Weight. Indones J Chem. 2022; 20(3): 722-728 https://doi.org/10.22146/ijc.44659.

13. Yakovenko O S, Magnetic anisotropy of the graphite nanoplatelet–epoxy and MWCNT–epoxy composites with aligned barium ferrite filler. J Mater Sci.2017; 52(9): 5345-5358. https://doi.org/10.1007/s10853-017-0776-4

14. Contri G, Barra GM, Ramoa SD, Merlini C, Ecco LG, Souza FS, et al, Epoxy coating based on montmorillonite-polypyrrole: Electrical properties and prospective application on corrosion protection of steel. Prog Org Coat. 2018; 114: 201-207. https://doi.org/10.1016/j.porgcoat.2017.10.008

15. Mohammed R, Saleh K. A novel conducting polyamic acid/nanocomposite coating for corrosion protection. Eurasian Chem Commun. 2021; 3: 715-725. https://doi.org/10.22034/ECC.2021.296065.1206

16. Ayat MA, Khlood AS. Electrochemical Polymerization of Eugenol and Corrosion Protection Studies of Stainless Steel 304L Alloy. J Med Chem Sci. 2023; 6: 1818-1829. https://doi.org/10.26655/JMCHEMSCI.2023.8.10

17. Kubba R M, Mohammed M A, Ahamed L S. DFT Calculations and Experimental Study to Inhibit Carbon Steel Corrosion in Saline Solution by Quinoline-2-One Derivative. Baghdad Sci J. 2021; 18(1): 113-123. https://doi.org/10.21123/bsj.2021.18.1.0113 .

18. Molaei M, Fattah-alhosseini A, Nouri M, Mahmoodi P, Navard S H, Nourian A. Enhancing cytocompatibility, antibacterial activity and corrosion resistance of PEO coatings on titanium using incorporated ZrO2 nanoparticles. Surf Interfaces, 2022; 30: 101967. https://doi.org/10.1016/j.surfin.2022.101967.

19. Li Z, Yuan X, Sun M, Li Z, Zhang D, Lei Y, et al. Rhamnolipid as an eco-friendly corrosion inhibitor for microbiologically influenced corrosion. Corros Sci. 2022; 204: 110390. https://doi.org/10.1016/j.corsci.2022.110390.

20. Mohammed M A, Kubba R M. Experimental Evaluation for the Inhibition of Carbon Steel Corrosion in Salt and Acid Media by New Derivative of Quinolin-2-One. Iraqi J Sci. 2020; 61(8) : 1861-1873. https://doi.org/10.24996/ijs.2020.61.8.2

21. Jassim R A, Farhan A M, Ali A M. Corrosion protection study of carbon steel and 316 stainless steel alloys coated by nanoparticles. Baghdad Sci. J. 2014;11(1):116-122. https://doi.org/10.21123/bsj.2014.11.1.116-122.

22. Abu Hassan Shaari H, Ramli M M, Mohtar M N, Abdul Rahman N, Ahmad A. Synthesis and conductivity studies of poly (Methyl Methacrylate)(PMMA) by co-polymerization and blending with polyaniline (PANi). polymer. 2021; 13(12): 1939.

23. Kubo I, Fujita KI, Nihei KI. Antimicrobial activity of anethole and related compounds from aniseed. J Sci Food Agric. 2008; 88(2): 242-7. https://doi.org/10.1002/jsfa.3079

24. Farag Z R, Moustapha M E, Abd El-Hafeez G M . The inhibition tendencies of novel hydrazide derivatives on the corrosion behavior of mild steel in hydrochloric acid solution. J Mater Res Technol. 2022; 16: 1422-1434. https://doi.org/10.1016/j.jmrt.2021.12.035.

25. Iman M M. Experimental and Quantum Chemical Studies on the Corrosion Inhibition of Mild Steel By 2-((Thiophen-2-Ylmethylene) Amino) Benzenethio in 1M HCl. Baghdad Sci J. 2019: 16(1): 49-55. https://doi.org/10.21123/bsj.2019.16.1.0049.

26. Abdulridha AA, Allah MA, Makki SQ, Sert Y, Salman HE, Balakit AA et al. Corrosion inhibition of carbon steel in 1 M H2SO4 using new Azo Schiff compound: electrochemical, gravimetric, adsorption, surface and DFT studies. J Mol Liq. 2020; 315: 113690. https://doi.org/10.1016/j.molliq.2020.113690.

27. Jiang Y, Zheng W, Tran K, Kamilar E, Bariwal J, Ma H, et al. Hydrophilic nanoparticles that kill bacteria while sparing mammalian cells reveal the antibiotic role of nanostructures. Nat Commun. 2022; 197(13) : 1-17. https://doi.org/10.1038/s41467-021-27193-9

28. Wang Y, Chen T, Wang H, Hu J, Ma Y, Wei J, et al. Corrosion inhibition effect of zeolitic imidazolate framework in chloride-contaminated cement pore solution under elevated temperatures. Constr Build Mater. 2022; 342: 128024. https://doi.org/10.1016/j.conbuildmat.2022.128024.

29. Almashhadani HA, Alshujery MK, Khalil M, Kadhem MM, Khadom AA. Corrosion inhibition behavior of expired diclofenac Sodium drug for Al 6061 alloy in aqueous media: Electrochemical, morphological, and theoretical investigations. J Mol

Liq. 2021; 343: 117656. https://doi.org/10.1016/j.molliq.2021.117656.

تأثير الكرافين واوكسيد الحديدوزعلى كفاءة طلاء البوليوجينول للفولاذ المقاوم للصدأ في محلول كلوريد الصوديوم

خلود عبد صالح ، ايات منذر القدسي

قسم الكيمياء، كلية العلوم، جامعة بغداد ، بغداد، العراق.

الخلاصة

التآكل هو مصطلح يطلق على عملية تفكك سطح المعادن والسبائك في بيئة معينة. تتغير الخواص الكيميائية للسبائك المعدنية بعد عملية التآكل وكذلك سلوكها الميكانيكي. لغرض الحماية من التآكل تم تطبيق إستراتيجية جديدة تعتمد على تخليق مادة بوليميرية من خلال البلمرة الكهربائية لليوجينول لتكوين للبولي يوجينول /المركب النانوي (Graphgene، Fe_3O_4)على الفولاذ المقاوم للصدأ نوع (SS316L) ، والذي يربط كقطب كهربائي انود ، باستخدام عملية البلمرة الكهربائية ، فإن البوليمر الموصل الناتج يعطي حماية جيدة ضد التآكل. تم اجراء الفحوصات المختبرية من التشخيص بتقنية الاشعة التحت الحمراء ومطيافية القوة الذرية للبوليمر المحضر لوحده مرة ومع المواد النانوية مرة اخرى. أظهرت النتائج أنه بالمقارنة مع SS316L الغير مطلي ، يوفر البولي يوجينول مع الكرافين أفضل حماية للمعدن المستخدم من التآكل.

الكلمات المفتاحية: يوجينول ,التآكل , بلمرة كهربائية ,مركبات نانوية ,بولي يجينول.